


## RESEARCH ARTICLE

# Discrimination of Regioisomeric and Stereoisomeric Saponins from *Aesculus hippocastanum* Seeds by Ion Mobility Mass Spectrometry

Emmanuel Colson,<sup>1,2</sup> Corentin Decroo,<sup>1,2</sup> Dale Cooper-Shepherd,<sup>3</sup> Guillaume Caulier,<sup>2</sup> Céline Henoumont,<sup>5</sup> Sophie Laurent,<sup>5</sup> Julien De Winter,<sup>1</sup> Patrick Flammang,<sup>2</sup> Martin Palmer,<sup>3</sup> Jan Claereboudt,<sup>4</sup> Pascal Gerbaux<sup>1</sup> 

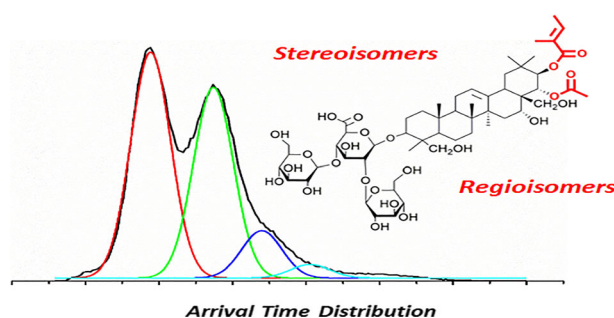
<sup>1</sup>Organic Synthesis and Mass Spectrometry Laboratory (S2MOs), University of Mons, 23 Place du Parc, 7000, Mons, Belgium

<sup>2</sup>Biology of Marine Organisms and Biomimetics Unit (BOMB), University of Mons, 23 Place du Parc, 7000, Mons, Belgium

<sup>3</sup>Waters Corporation, Altrincham Road, Wilmslow, SK9 4AX, UK

<sup>4</sup>Waters Corporation, Brusselsesteenweg 500, 1731, Zellik, Belgium

<sup>5</sup>Department of General, Organic and Biomedical Chemistry, NMR and Molecular Imaging Laboratory, University of Mons, 23 Place du Parc, 7000, Mons, Belgium



**Abstract.** Modern mass spectrometry methods provide a huge benefit to saponin structural characterization, especially when combined with collision-induced dissociation experiments to obtain a partial description of the saponin (ion) structure. However, the complete description of the structures of these ubiquitous secondary metabolites remain challenging, especially since isomeric saponins presenting small differences are often present in a single extract. As a typical

example, the horse chestnut triterpene glycosides, the so-called escins, comprise isomeric saponins containing subtle differences such as cis-trans ethylenic configuration (stereoisomers) of a side chain or distinct positions of an acetyl group (regioisomers) on the aglycone. In the present paper, the coupling of liquid chromatography and ion mobility mass spectrometry has been used to distinguish regioisomeric and stereoisomeric saponins. Ion mobility arrival time distributions (ATDs) were recorded for the stereoisomeric and regioisomeric saponin ions demonstrating that isomeric saponins can be partially separated using ion mobility on a commercially available traveling wave ion mobility (TWIMS) mass spectrometer. Small differences in the ATD can only be monitored when the isomeric saponins are separated with liquid chromatography prior to the IM-MS analysis. However, gas phase separation between stereoisomeric and regioisomeric saponin ions can be successfully realized, without any LC separation, on a cyclic ion mobility-enabled quadrupole time-of-flight (Q-cIM-oeToF) mass spectrometer. The main outcome of the present paper is that the structural analysis of regioisomeric and stereoisomeric natural compounds that represents a real challenge can take huge advantages of ion mobility experiments but only if increased ion mobility resolution is attainable.

Published online: 26 August 2019

**Keywords:** Saponins, Ion mobility, Cyclic ion mobility, TWIMS, Stereoisomers, Regioisomers, Natural products, Escin

**Electronic supplementary material** The online version of this article (<https://doi.org/10.1007/s13361-019-02310-7>) contains supplementary material, which is available to authorized users.

Received: 26 March 2019/Revised: 1 August 2019/  
Accepted: 8 August 2019

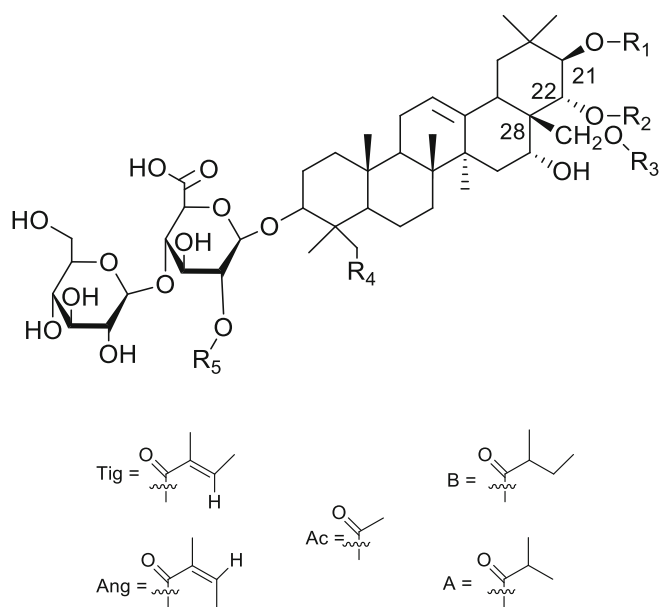
Correspondence to: Pascal Gerbaux; e-mail: [pascal.gerbaux@umons.ac.be](mailto:pascal.gerbaux@umons.ac.be)

Published online: 26 August 2019

## Introduction

Saponins are amphiphilic molecules of pharmaceutical interest and most of their biological activities (i.e., cytotoxic, hemolytic, fungicide...) are associated with their membranolytic properties [1–3]. These molecules are secondary metabolites present in numerous plants [4–6] and in some marine animals, such as sea cucumbers [7–9] and starfishes [10–12]. Structurally, all saponins correspond to the combination of a hydrophilic glycone, consisting of one (or more) sugar chain, linked to a hydrophobic triterpenoidic or steroidal aglycone, named the sapogenin [13, 14]. Saponin congeners can be roughly classified according to the number of saccharidic chains appended to the aglycone moiety. Monodesmosidic saponins are characterized by the condensation of a single oligosaccharide onto the aglycone, whereas polydesmosidic structures are defined when several oligosaccharide chains are grafted onto the aglycone. Due to their huge structural diversity, the structural characterization of saponins remains challenging and the development of efficient analytical methods is a perpetual task. Structure elucidation of saponins by mass spectrometry (MS) has been widely reported in the recent literature and the application of state-of-the-art MS methods, such as LC-MS(MS) and MALDI-MS(MS), has helped in resolving complex mixtures of saponins from natural extracts [6, 7, 9, 11, 15, 16]. Recently, ion mobility spectrometry (IMS) [17, 18] was introduced into the toolbox for MS-based saponin characterization [19]. Structural characterization using IMS relies on the comparison of the measured collisional cross sections ( $CCS_{exp}$ ) with theoretical values ( $CCS_{th}$ ) calculated using dedicated software, such as Mobcal, for candidate structures generated by molecular dynamics (MD) simulations [17, 18]. A broad structural selection of saponin molecules, in terms of the number of saccharide units and their topology, including monodesmosidic and bidesmosidic saponins, has been sampled. The  $[M+H]^+$ ,  $[M+Na]^+$ , and  $[M+K]^+$  saponin ions have been analyzed by IMS in order to obtain experimental CCS and to perform MD simulations to generate candidate ion structures [19, 20]. From these studies, the IMS/MD combination, while powerful, cannot be considered as a universal or stand-alone method for saponin characterization [19, 20]. As a striking example, even for chromatography-resolved (i.e., liquid chromatography) saponin isomers, the differences observed in CCS are too small to carry straightforward structural information [20]. Based on molecular dynamics simulation, the ionization of the saponin molecules was shown to induce the folding of the saponin molecule around the charge site, concealing small structure differences within a compact global 3D ion structure [20]. However, as an encouraging result, different saponin ions can present distinct experimental CCSs [19]. This is especially remarkable when the distinction between monodesmosidic and bidesmosidic saponins is considered. Indeed, the  $[M+Na]^+$  bidesmosidic ions always appear significantly more compact than their  $[M+H]^+$  homologues (about 10% CCS reduction) whereas, for the monodesmosidic molecules, the CCS are almost identical for the  $[M+H]^+$  and  $[M+Na]^+$  ions [19].

In this work, the ability of IMS to discriminate regioisomeric and stereoisomeric saponins will be evaluated. Specifically, the saponins contained in horse chestnut (HC) seeds have been selected and analyzed. HC saponins are a mixture of triterpenoid saponins, the well-known  $\alpha$ - and  $\beta$ -escins [21–25]. These molecules, especially the  $\beta$ -escins, are widely used in Chinese medicine to cure numerous diseases. Previous studies have already highlighted the potential of saponins as anti-inflammatory, antiseptic, antipyretic agents or to be effective against digestive disorders [25, 26]. As presented in Scheme 1, these molecules are based on a protoescigenin (sapogenin) substituted in C-3, C-21, C-22, and C-28 by different side chains. The glycone moiety, attached in C-3 on the aglycone, is invariably a branched trisaccharide that always integrates a conserved glucuronic acid-glucose sequence, whereas the third monosaccharide residue is variable (glucose, xylose, or galactose) [23, 24]. As presented in Scheme 1 and Tables 1 and SI1, the escin family comprises several molecules that are structurally distinguished also based on the nature of the side chains in C-21 ( $R_1$ ), C-22 ( $R_2$ ), and C-28 ( $R_3$ ). In C-21, among the different side chains, tiglic acid (Tig) and angelic acid (Ang) residues are of prime interest for the present study since they are only differentiated based on the *cis-trans* configuration of the C=C bond. For instance, escin 1a and escin 1b are stereoisomeric saponins distinguished based on the terminology *a/b*, with *a/b* corresponding to *Tig/Ang* (Scheme 2). In addition, escin congeners are also classified into two series of  $\alpha$  and  $\beta$  isomers [21] defined by the presence of an acetyl group at C-22 or C-28, respectively (Scheme 2).  $\beta$ -Escins, the major active component in extracts of HC, are primarily composed of escin 1a and escin 1b [23], while  $\alpha$ -escins are mainly composed of isoescin 1a and isoescin 1b [23]. Then, escin 1a and isoescin 1a are regioisomeric saponins, as are escin 1b and isoescin 1b



**Scheme 1.** Molecular structures of the escin molecules. Tig, Ang, and Ac stand for tiglic acid, angelic acid, and acetic acid, respectively (see Table 1 for more details)

**Table 1.** LC-IMS-MS (Waters Synapt G2-Si) Analysis of the Horse Chestnut Saponin Extract: Accurate Mass Measurements (Mass Error), Retention Time (RT) and Arrival Times ( $t_A$ ). The Collisional Cross Sections (CCS) of  $[M+Na]^+$  Ions Are Determined Using the Calibration Procedure from Reference [27]

	Composition	$m/z$ $[M+Na]^+$	$R_1$	$R_2$	$R_3$	$R_4$	$R_5$	RT (min)	$t_A$ $[M+Na]^+$	CCS $[M+Na]^+$
Escin 1a	$C_{55}H_{86}O_{24}$	1153.5407 (1.8)	–Tig	–Ac	–H	–OH	–Glc	6.9	9.83	308
Escin 1b			–Ang	–Ac	–H	–OH	–Glc	7.13	9.75	306
Isoescin 1a			–Tig	–H	–Ac	–OH	–Glc	7.25	9.97	311
Isoescin 1b			–Ang	–H	–Ac	–OH	–Glc	7.44	9.83	308
Escin 2a	$C_{54}H_{84}O_{23}$	1123.5301 (0.9)	–Tig	–Ac	–H	–OH	–Xyl	6.86	9.35	298
Escin 2b			–Ang	–Ac	–H	–OH	–Xyl	7.1	9.28	296
Isoescin 2a			–Tig	–H	–Ac	–OH	–Xyl	7.26	9.49	301
Isoescin 2b			–Ang	–H	–Ac	–OH	–Xyl	7.44	9.35	298
Escin 3a	$C_{55}H_{86}O_{23}$	1137.5458 (1.4)	–Tig	–Ac	–H	–H	–Gal	7.25	9.9	309
Escin 3b			–Ang	–Ac	–H	–H	–Gal	7.49	9.83	308
Escin 4	$C_{52}H_{82}O_{24}$	1113.5094 (1.3)	–Ac	–Ac	–H	–OH	–Glc	4.77	9.14	294
Isoescin 4			–Ac	–H	–Ac	–OH	–Glc/Gal	5.26	9.14	294
Escin 5	$C_{54}H_{86}O_{24}$	1141.5407 (2.2)	–A	–Ac	–H	–OH	–Glc	6.54	9.7	305
Escin 6	$C_{55}H_{88}O_{24}$	1155.5411 (4.1)	–B	–Ac	–H	–OH	–Glc	7.44	9.83	308
Escin 7	$C_{51}H_{80}O_{23}$	1083.4988 (2.3)	–Ac	–Ac	–H	–OH	–Xyl	4.72	8.73	285
Isoescin 7			–Ac	–H	–Ac	–OH	–Xyl	5.24	8.66	283
Escin 8	$C_{53}H_{84}O_{23}$	1111.53 (0.3)	–A	–Ac	–H	–OH	–Xyl	6.53	9.42	299
Escin 9	$C_{52}H_{82}O_{23}$	1097.5145 (0.5)	–Ac	–Ac	–H	–H	–Glc/Gal	5.22	9.14	294

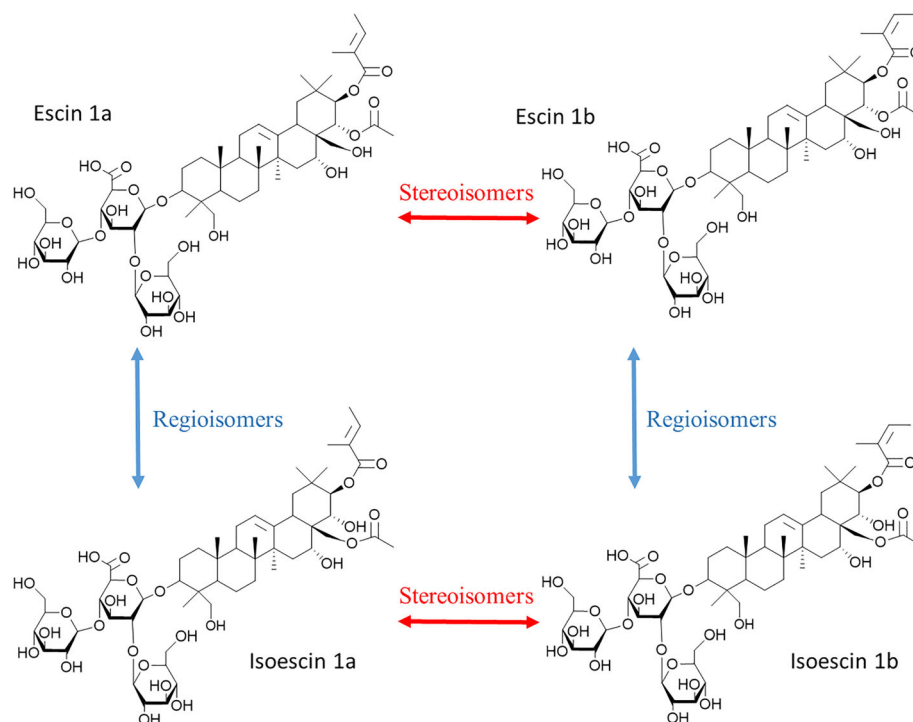
and the prefix *iso* is used in nomenclature to distinguish regioisomers (Scheme 2).

In the present study, all the saponins extracted from the HC seeds will be submitted to LC-IMS experiments and their arrival time distributions (ATDs) will be recorded with and without liquid chromatography separation to evaluate whether IMS can discriminate stereoisomeric or regioisomeric saponins.

## Experimental

### Chemicals, Plant Sampling, and Saponin Extractions

**Chemicals** For saponin extractions and mass spectrometry analyses, technical grade methanol, hexane, dichloromethane, chloroform, and isobutanol, as well as HPLC grade water, acetonitrile, and methanol, were purchased from CHEM-LAB NV (Somme-Leuze, Belgium). *N,N*-Dimethylaniline (DMA) and 2,5-dihydroxybenzoic acid (DHB) were provided by Sigma-Aldrich (Diegem, Belgium).

**Scheme 2.** Nature of the isomeric relations between escin 1a, escin 1b, isoescin 1a, and isoescin 1b

**Sampling** HC tree seeds (*Aesculus hippocastanum*) were picked up by hand in September 2017 in Mons, Belgium (50° 27' 32.4" N, 3° 57' 38.5" E). The seeds were first summarily ground with a hammer and were oven-dried at 50 °C overnight. The dried fragments were powdered with an IKA crusher and immediately submitted to the extraction procedure.

**Saponin Extraction** The powder underwent an extraction method adapted from a previously published procedure, Van Dyck et al. [16]. The weighed powder is stirred in methanol during 24 h at room temperature followed by filtration. The extract is diluted to 70% methanol with water mQ. The solution is partitioned (v/v) successively against *n*-hexane, dichloromethane, and chloroform. Finally, the hydromethanolic solution is evaporated at low pressure in a double boiler at 46 °C using a rotary evaporator. The dry extract is diluted in water to undergo a last partitioning against isobutanol (v/v). The butanolic phase is washed twice with water to remove salts and impurities. This organic solution contains the saponins.

**Liquid Chromatography and Ion Mobility Mass Spectrometry Analyses** Ion mobility measurements were performed using a hybrid quadrupole (Q)—traveling wave ion mobility (TWIMS)—time-of-flight (ToF) mass spectrometer (SYNAPT G2-Si, Waters, UK). The ion mobility separation stage of the instrument is constituted by the so-called tri-wave setup that is composed of three successive T-wave devices, described as the trap cell, the IMS cell, and the transfer cell, in which the TWIMS velocity and amplitude are user-tuneable. The trap and transfer cells are filled with argon whereas the IMS cell is filled with nitrogen. A small rf-only cell filled with helium is fitted between the trap and the IMS cells. Collision energy can be applied to the trap cell and to the transfer cell to fragment ions before and after the ion mobility separation. The typical IMS parameters are as follows: wave height 40 V, wave velocity 400 m s<sup>-1</sup>, nitrogen IMS flow 110 mL min<sup>-1</sup>, helium cell gas flow 180 mL min<sup>-1</sup>, trap CE 4 V, transfer CE 2 V, and trap bias 30 V. TWIMS data were analyzed using Waters MassLynx SCN 901 software. ATDs were extracted using Waters MassLynx by selecting the most abundant isotope for each ion composition to avoid unspecific selection. Arrival times (*t<sub>A</sub>*) are then determined at the maximum of the ATD and are converted into collisional cross section (CCS) values in helium by means of the polymer calibration described in ref. [27] using commercial PEG samples with average molecular weights of 600, 1000, and 2000.

**Cyclic Ion Mobility Mass Spectrometry Analyses** Further studies were performed on a cyclic ion mobility (cIM) enabled quadrupole time-of-flight (Q-cIM-oaToF) mass spectrometer (Waters, UK) [28, 29]. This system has a similar geometry to the SYNAPT G2-Si, with a trap cell proceeding the cIM device, followed by a transfer cell and an oaToF operating at

resolutions of up to 100,000 FWHM (full width at half maximum).

The cIM device has multiple benefits: the circular path minimizes instrument footprint while providing a longer, higher mobility resolution separation path; a multi-pass capability provides significantly higher resolution (> 500 CCS/ΔCCS) over a reduced (selected) mobility range; the device can be enabled for mobility separation or by-passed if not required and, the multifunctional ion entry/exit array can selectively eject species within a range of mobilities, providing additional functionality. The cIM device consists of a 100-cm path length RF ion guide comprising over 600 electrodes around which T-waves circulate to provide mobility separation.

To control the cIM device, cyclic sequence methods were created to allow time resolved manipulation of the ions—these methods included steps such as “inject,” “separate,” “eject to store,” “re-inject from store,” and “eject and acquire”—by varying the sequence and the associated time for each step complex ion manipulation experiments can be designed. Three sequences were created for this investigation:

1. Quad isolation of *m/z* 1153 [M+Na]<sup>+</sup> ion, trap CE 40 V (to reduce dimer intensity), and 15 passes of the cIM device prior to ToF separation
2. Quad isolation of *m/z* 1153 [M+Na]<sup>+</sup> ion, trap CE 80 V (to generate *m/z* 653 fragment ion) and 10 passes of the cIM device prior to ToF separation
3. Quad isolation of *m/z* 1153 [M+Na]<sup>+</sup> ion, trap CE 80 V (to generate *m/z* 653 fragment ion), and 10 passes of the cIM device followed by transfer CE 40 V (to generate mobility aligned second-generation fragment ions) prior to ToF separation

The ion mobility resolution scales with the square root of the number of passes of the cIM device, 15 passes corresponds to a resolution of ~250 CCS/ΔCCS, and 10 passes equates to ~200 CCS/ΔCCS.

The typical IMS parameters were as follows: wave height 45 V, wave velocity 375 m s<sup>-1</sup>, nitrogen IMS flow 25 mL min<sup>-1</sup>, helium cell gas flow 120 mL min<sup>-1</sup>, trap CE 40 V, and transfer CE 0 V. Nitrogen was used for collision and IMS gas. Data were analyzed using a development version of Waters MassLynx software. ATDs are extracted using Waters Driftscope mobility visualisation software and MassLynx by selecting the most abundant isotope for each ion composition to avoid unspecific selection.

## Results and Discussion

The HC saponin extract is first analyzed by a global method for saponin characterization by combining MALDI-ToF, LC-MS, and collision-induced dissociation experiments (CID/MSMS) [20] to (i) determine the *m/z* ratios of saponin ions (and the elemental compositions of the corresponding saponins by



accurate mass measurements) from the MALDI-ToF experiments, (ii) evaluate the presence of isomers by LC-MS by monitoring the retention times, and (iii) establish the primary structures of saponin ions upon CID by identifying structure-specific fragmentation pathways. As detailed in the Supplementary Information, based on these MALDI and LC-MSMS experiments, nine different saponin compositions are observed for a total of 18 saponin molecules (see Table SI 1). Interestingly, compared to the literature, we succeeded in detecting two new elemental compositions and six new saponins.

### *TWIMS Experiments on Ionized HC Saponins*

The HC extract is analyzed by LC-IMS-MS on a Waters SYNAPT G2-Si mass spectrometer and the ATDs of all the saponin ions,  $[M+Na]^+$ , are recorded in the positive ion mode. The saponin molecules presented in Table 1 are detected in the saponin extract and are resolved using liquid chromatography as shown in Figure 1a for the typical case of escin 1 isomers. The structural assignment of the LC peaks is achieved based upon the mass spectrometry data together

with nuclear magnetic spectrometry (NMR) experiments on isolated saponins (see SI for more details). Table 1 also gathers the arrival times ( $t_A$ ) of the  $[M+Na]^+$  ions. As reported in a previous investigation concerning saponin ion mobility [20], the  $t_A$  are quite similar for isomeric ions presenting only subtle structural differences. For instance, the  $t_A$  of the  $[M+Na]^+$  ions generated from the four isomeric escin 1 saponins are measured at 9.83, 9.75, 9.97, and 9.83 ms respectively for escin 1a, escin 1b, isoescin 1a, and isoescin 1b (Table 1 and Figure 1b). The Tig-containing saponins appear less compact than the Ang-containing counterparts, 9.83 ms vs 9.75 ms (escin 1a vs escin 1b) and 9.97 vs 9.83 ms (isoescin 1a vs isoescin 1b) for the  $[M+Na]^+$  ions. The regioisomer separation of the  $[M+Na]^+$  ions of escin 1a and escin 1b are characterized by shorter  $t_A$  than their isoescin 1a and isoescin 1b regioisomers. However, escin 1a and isoescin 1b that are both regioisomers and stereoisomers cannot be separated using ion mobility (Figure 1b and Table 1). The same discussion holds for the different sets of isomers as presented in Table 1.

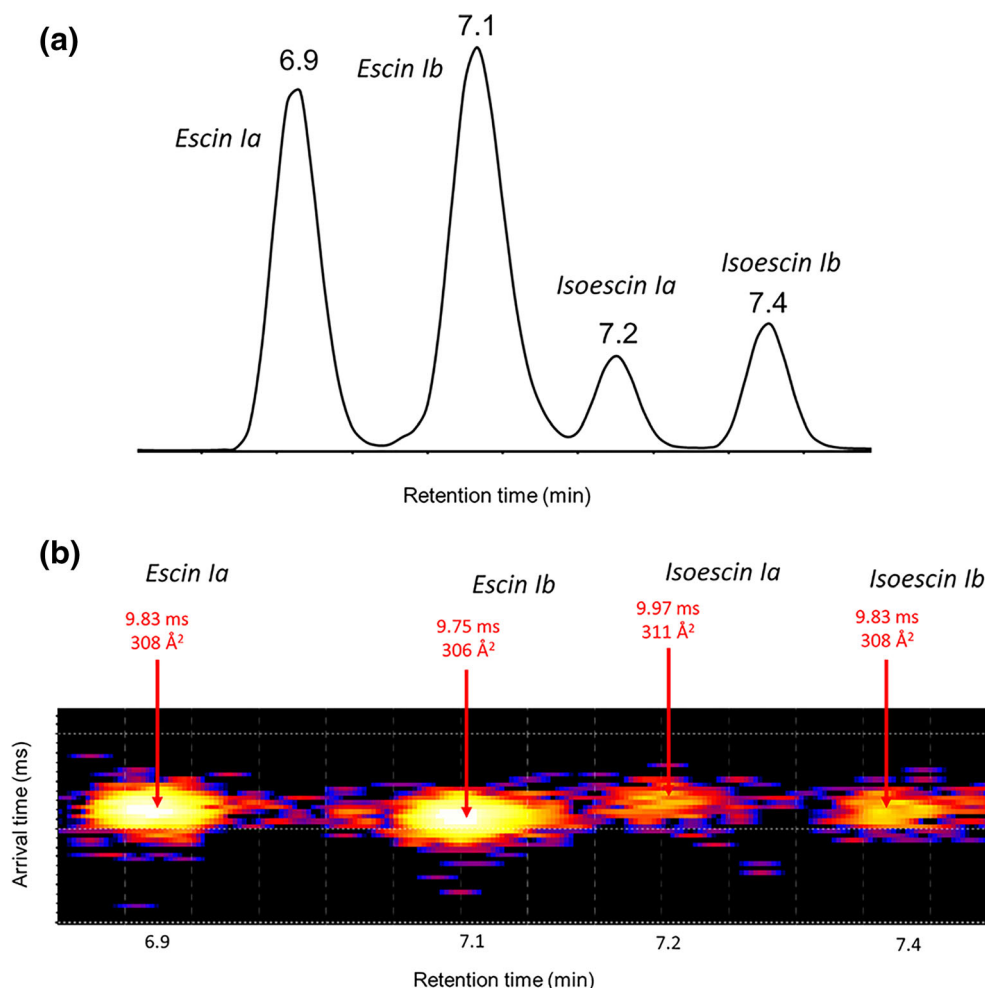


**Figure 1.** LC-IMS-MS analysis of the horse chestnut saponin extract: (a) extracted ion current (EIC) of the  $m/z$  1153.5  $[M+Na]^+$  ions and (b) arrival time vs retention time plot for the four escin 1 isomers (see the experimental section for the LC-MS conditions)

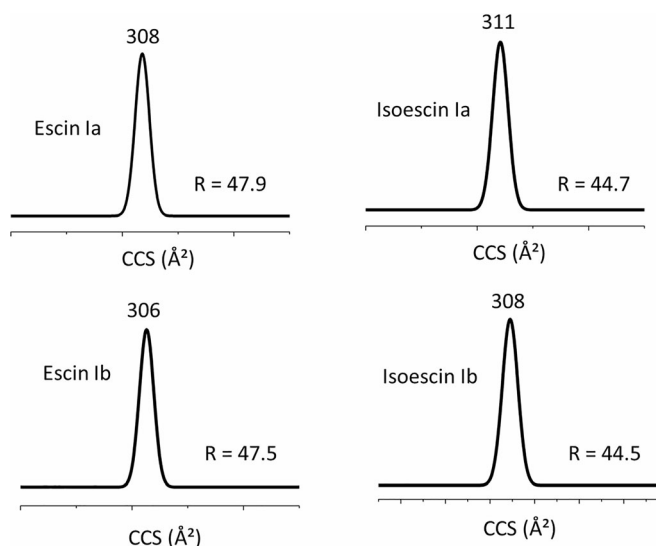


**Figure 2.** LC-IMS analysis (Waters Synapt G2-Si) of the horse chestnut saponin extract: collisional cross section (CCS) distributions for the  $[M+Na]^+$  ions of the escin 1 isomers.  $R$  corresponds to the CCS resolution calculated by  $R_{CCS} = CCS / \Delta CCS(50\%)$

Ion mobility data are often converted to collisional cross sections (CCS) to confer a structural dimension to the IMS data [30]. Indeed, where the  $ATD/t_A$  clearly depend on the experimental conditions (gas flow and nature, wave velocity, and height on a TWIMS setup,...), the CCS data characterize the gas/ion interaction [30]. The CCS of all the  $[M+Na]^+$  saponin ions have been determined and are presented in Table 1. ATDs are converted into collisional cross section (CCS) values in helium by means of the polymer calibration described in ref. [28, 29]. Commercial instruments are usually used with  $N_2$  in the mobility cell, although CCS obtained in He are preferable for correlation with future theoretical calculations [18]. Each CCS distribution is characterized by a CCS resolution— $R_{CCS}$ —that is defined as the  $CCS/\Delta CCS$  (FWHM) [31, 32]. As for a typical example, the CCS distributions of the four isomers of escin 1 are plotted in Figure 2. The CCS distributions are nearly superimposable, and the

presented data can be only resolved due to the liquid chromatography step preceding the IM-MS analysis (Figure 1a). Interestingly, the resolution of the CCS distributions is close to the expected theoretical IM resolution ( $\sim 40$ ) expected for the TWIMS setup of the Waters SYNAPT G2-Si mass spectrometer [32]. This clearly demonstrates that higher CCS resolution instruments are required from an analytical point of view, especially if no LC separation precedes the ion mobility separation.

### *Cyclic Ion Mobility Experiments on Ionized Escin 1a, Escin 1b, Isoescsin 1a, and Isoescsin 1b*

The HC extract was then analyzed by direct infusion (no LC separation) on a cyclic ion mobility system. This cyclic TWIMS device is characterized by a scalable resolution, ranging from 65 (1 pass) upwards depending on the number of passes/cycles (between 1 and 15 passes  $R \sim 65$  and 250 as used in this study). The IMS resolution increases with the square root of the number of passes (length) [28, 29]. As presented in Figure 3, the  $[M+Na]^+$  ions ( $m/z$  1153.5) of the four escin 1 isomers are not separated by cIM with one pass, whereas, after 15 passes, two major overlapping signals are recorded at 349.4 and 353.6 ms, with some tailing above 360 ms. The ATD recorded upon direct infusion can be deconvoluted into four different contributions, as presented in Figure 3b. Doing so, we theoretically determined the  $t_A$  at 349.4 ms, 353.6 ms, 357.4 ms, and 360.1 ms, respectively, for the  $[M+Na]^+$  ions of escin 1a, escin 1b, isoescsin 1a, and isoescsin 1b. This mobility separation correlates with the  $t_A$  (Table 1) and the CCS (Figure 2) measured on the SYNAPT G2-Si using linear TWIMS, escin 1b ions (9.75 ms, 306 Å<sup>2</sup>), escin 1a ions, isoescsin 1b ions (9.83 ms, 308 Å<sup>2</sup>), and isoescsin 1a ions (9.97 ms, 311 Å<sup>2</sup>). The highest resolution used with the cIM device allows slight separation of the escin 1a and isoescsin 1b ions that were previously not distinguished during the linear TWIMS experiments (see Table 1 and Figure 2).

When running LC-cIM-MS experiments (see Figure 4) [28, 29], it is possible to measure the  $t_A$  of the separated escin ions at about 355 ms ( $t_A$  from deconvolution in Figure 3b, 353.6 ms),

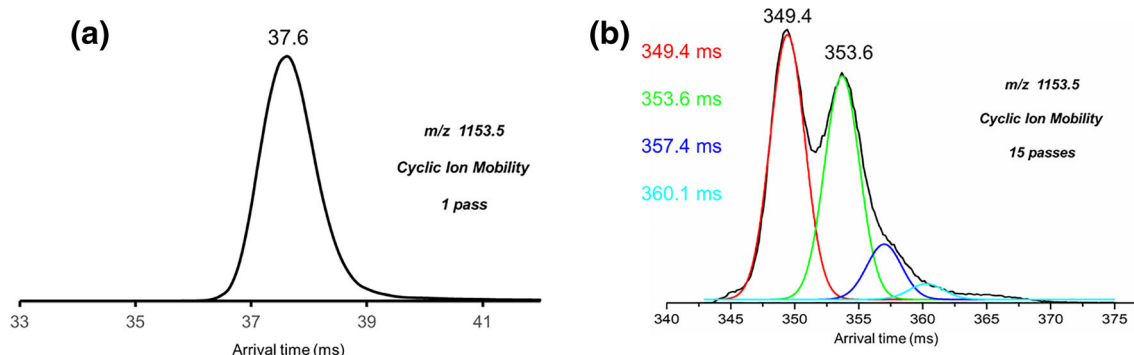


**Figure 3.** ESI-cIM-MS analysis—direct infusion—of the horse chestnut saponin extract: arrival time distributions (ATD) for the  $[M+Na]^+$  ions of the escin 1 isomers ( $m/z$  1153.5): (a) 1 pass and (b) 15 passes. Note that the  $m/z$  1153.5 ions are mass-selected by the quadrupole analyzer prior the cIM separation. In (b), the deconvolution is performed using Origin 9.0 by imposing the same width for the Gaussian curves

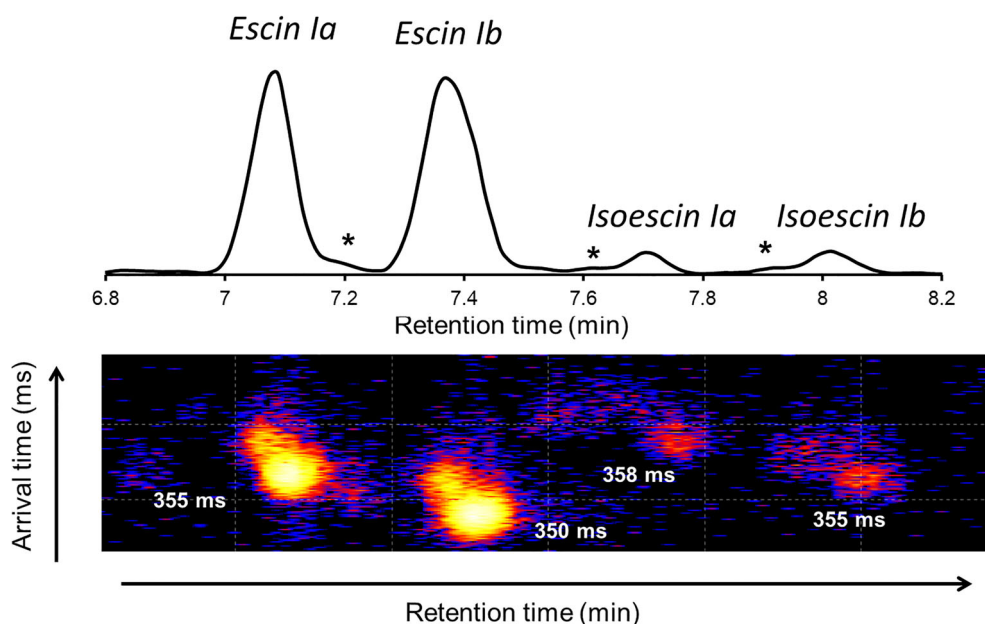


**Figure 4.** LC-cIM-MS analysis (15 passes) of the horse chestnut saponin extract: extracted ion current chromatograms ( $m/z$  1153.5) and arrival time vs retention time plot for the  $[M+Na]^+$  ions of the escin 1 isomers ( $m/z$  1153.5). Note that the  $m/z$  1153.5 ions are mass-selected by the quadrupole analyzer prior to the cIM separation. Asterisk stands for isobaric contaminations

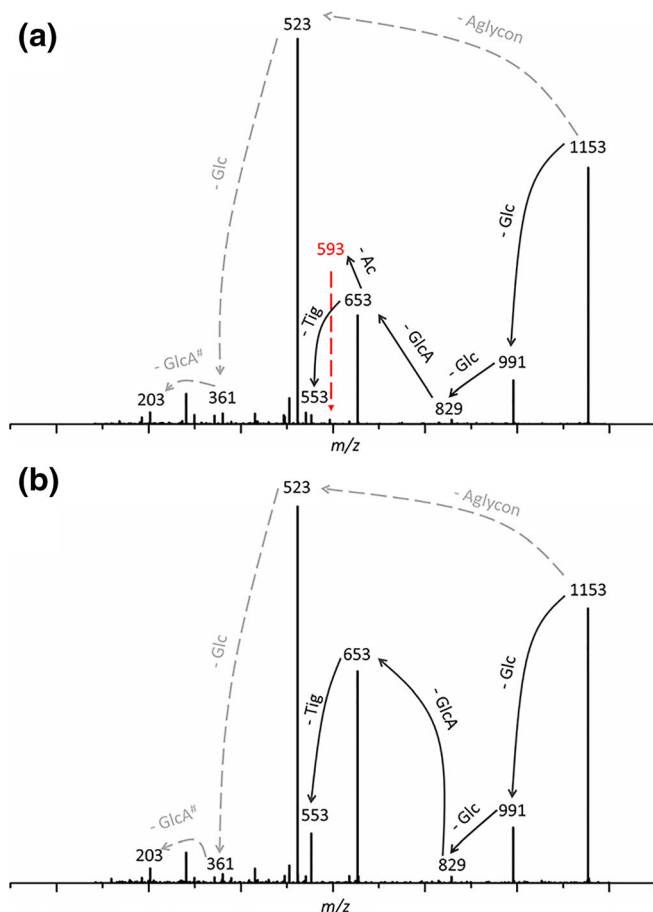


**Figure 5.** LC-MS/MS analyses of the horse chestnut saponin extract (Waters Synapt G2-Si): CID spectra of the  $[M+Na]^+$  ions ( $m/z$  1153.5) from (a) escin 1a and (b) isoescsin 1a

350 ms (349.4 ms), 358 ms (360.1 ms), and 355 ms (357.4 ms) for the  $[M+Na]^+$  ions of escin 1a, escin 1b, isoescsin 1a, and isoescsin 1b, respectively. These experimental data correlate nicely with the  $t_A$  determined upon deconvolution in Figure 3.

Observation of the molecular structures presented in Scheme 2 reveals that the distinction between the escin 1 isomers is contained in the aglycone units. Collision-induced dissociation experiments were subsequently used to fragment the  $m/z$  1153.5  $[M+Na]^+$  precursor ions from their trisaccharidic chains and expose the  $m/z$  653.5 fragment ions to the cIM separation. The CID spectra of the escin 1 isomers are presented in Figure 5 (see Figure SI 5 for all the CID spectra). Besides the dominant CID reaction leading to the trisaccharidic ions detected at  $m/z$  523, the loss of the oligosaccharide chain from the collisionally excited  $m/z$  1153 ions generate the  $m/z$  653.5 ions containing the stereoisomeric/regioisomeric information (see Scheme 2). The HC extract solution was then infused in the electrospray source and the  $m/z$  1153.5 ions mass-selected by the quadrupole analyzer. These ions were exposed to CID in the trap cell (trap CE at 80 V in nitrogen) to generate the  $m/z$  653.5 fragment ions that are consecutively subjected to cIM separation with an increasing number of passes (1 pass, 5 passes, and 10 passes). As presented in Figure 6, after one pass, no isomer separation is observed. Whereas five passes allow discrimination of three ion populations, with further passes, four ATD signals are unambiguously detected with a quasi-baseline separation when the  $m/z$  653.5 ions undergo a 10-pass separation. In other words, the four isomeric aglycone ions are discriminated upon cIM, without any LC separation.

Collisional activation of ions can also be achieved after ion mobility separation. Inspection of the CID spectra in

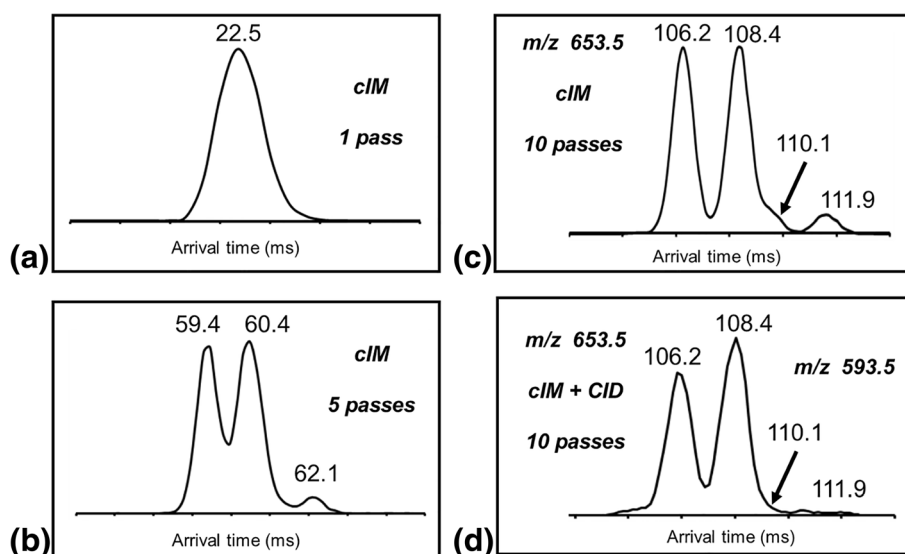
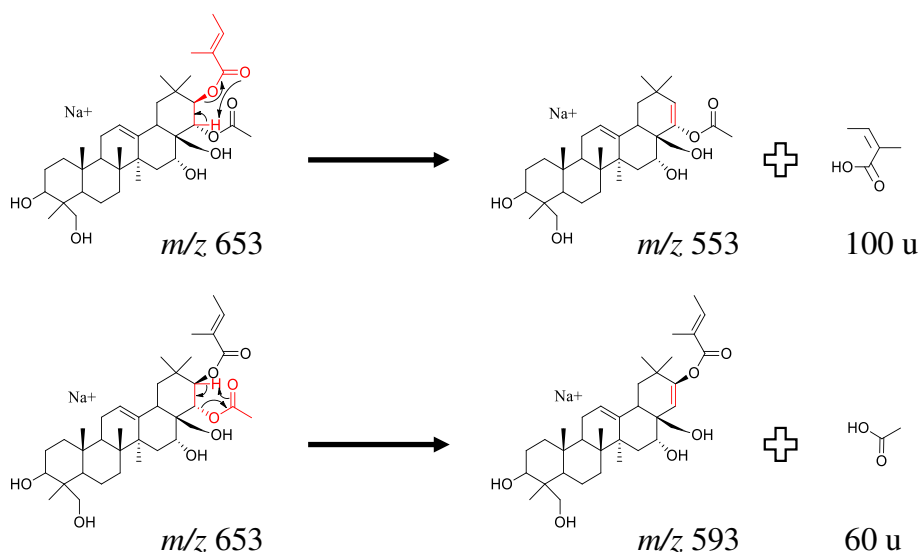


**Figure 6.** (a–c) ESI-cIM-MS analysis—direct infusion—of the horse chestnut saponin extract: arrival time distributions (ATD) for the  $m/z$  653.5 fragment ions generated by CID in the trap cell (trap CE = 80 V) from the mass-selected  $[M+Na]^+$  ions of the escin 1 isomers ( $m/z$  1153.5): observation of the increased cIM separation with the number of passes (1–5–10 passes). (d) ESI-cIM-CID<sub>transfer</sub>-MS analysis—direct infusion—of the horse chestnut saponin extract: relative abundances of the  $m/z$  593.5 fragment ions generated upon CID in the transfer cell (trap CE = 80 V) from the cIM-separated (10 passes)  $m/z$  653.5 precursor ions

Figure 5 reveals a subtle difference between the escin and the isoescsin  $[M+Na]^+$  ions. The  $[M+Na]^+$  precursor ions associated with escin 1a (and escin 1b) and isoescsin 1a (and isoescsin 1b) lose their oligosaccharide chains to produce the aglycone ions at  $m/z$  653.5. From these ions, a 100 u loss (tiglic or angelic acid) is observed for the four isomers (see Table SI 1), whereas the loss of acetic acid (60 u) is only observed for the isoescsin isomers. From Scheme 3, the 60 and 100 u losses can be associated with McLafferty rearrangements involving the breaking of the C–21–O and C–22–O bonds, respectively. Such a McLafferty rearrangement

is not feasible for the regioisomeric isoescsin 1a and 1b ions, since no  $\gamma$  hydrogen atom is present in agreement with the absence of the 60 u loss process.

Finally, we performed an experiment based upon the following sequence of events: direct infusion → mass selection of the  $m/z$  1153.5 precursor ions → CID in the trap cell to generate the  $m/z$  653.5 ions → cIM with 10 passes on all the ions generated in the trap cell → CID in the transfer cell → ToF mass measurement and detection. Such a sequence of experiments is referred as drift time-aligned CID experiments [33]. Whereas Figure 6c presents the ATD of the  $m/z$



**Scheme 3.** Collision-induced dissociation of the  $m/z$  653 aglycone ions from the  $[M+Na]^+$  ions of escin 1a: McLafferty rearrangements leading to the (a) 100 u loss and (b) 60 u loss



653.5 ions that have been generated in the trap cell from the  $m/z$  1153.5 ions, we plot in Figure 6d the relative abundances of the  $m/z$  593.5 ions generated upon CID of the  $m/z$  653.5 ions within the transfer cell. They exhibit the same cIM ATD signature as the precursor ions since they were generated downstream of the ion mobility device. From the comparison between Figure 6c and d, we can conclude that the  $m/z$  653.5 ions characterized by  $t_A$  at 110.1 and 111.9 ms marginally expel 60 u confirming thus that they correspond to the isoescins isomers.

## Conclusions

*Aesculus hippocastanum*, commonly known as the horse chestnut tree or conker tree, is a well-known large tree, abundantly cultivated in streets and parks in temperate countries, especially in Western Europe. Its seeds are well known to contain saponin congeners presenting different compositions and different structures. The HC saponin extract is particularly challenging from an analytical point of view since regioisomeric and stereoisomeric saponins are present. In the present paper, it has been shown that ion mobility experiments together with liquid chromatography separation can be utilized for the structural characterization of stereoisomeric and regioisomeric saponins. Saponins presenting isomeric side chains, such as tiglic and angelic acid residues, can be distinguished by recording the ATDs, provided that high-resolution ion mobility separation is used. This was demonstrated by comparing the capabilities of the Waters SYNAPT G2-Si mass spectrometer equipped with a conventional TWIMS device to an experimental cyclic ion mobility system (cIM) setup. Based on higher ion mobility resolution due to the multi-pass IMS<sup>n</sup> experiments and versatile fragmentation/spectrum clean-up/ion manipulation capabilities, we succeeded in discriminating stereoisomeric and regioisomeric natural molecules. The present work suggests that natural product analysis will benefit enormously from improvements in ion mobility techniques, in particular increased resolution.

## Acknowledgements

The MS laboratory acknowledges the “Fonds de la Recherche Scientifique (FRS-FNRS)” for its contribution to the acquisition of the Waters QToF Premier and the Waters SYNAPT G2-Si mass spectrometers. P.F. is Research Director of the FRS-FNRS. E.C. and C.D. are grateful to the F.R.I.A. for the financial support.

## References

- Lorent, J.H., Quetin-Leclercq, J., Mingot-Leclercq, M.P.: The amphiphilic nature of saponins and their effects on artificial and biological membranes and potential consequences for red blood and cancer cells. *Org. Biomol. Chem.* **12**, 8803–8822 (2014)
- Segal, R., Schlösser, E.: Role of glycosidases in the membranolytic, antifungal action of saponins. *Arch. Microbiol.* **104**, 147–150 (1974)
- Podolak, I., Galanty, A., Sobolewska, D.: Saponins as cytotoxic agents : a review. *Phytochem. Rev.* **9**, 425–474 (2010)
- Vincken, J.P., Heng, L., de Groot, A., Gruppen, H.: Saponins, classification and occurrence in the plant kingdom. *Phytochemistry*. **68**, 275–297 (2007)
- Sparg, S.G., Light, M.E., Van Staden, J.: Biological activities and distribution of plant saponins. *J. Ethnopharmacol.* **94**, 219–243 (2004)
- Madl, T., Sterk, H., Mittelbach, M., Rechberger, G.N.: Tandem mass spectrometric analysis of a complex triterpene saponin mixture of *Chenopodium quinoa*. *J. Am. Soc. Mass Spectrom.* **17**, 795–806 (2006)
- Bahrami, Y., Zhang, W., Franco, M.M.: C.: Distribution of saponins in the Sea Cucumber *Holothuria lessona*; the body wall versus the viscera, and their biological activities. *Mar. Drugs*. **16**, 423 (2018)
- Yamanouchi, T.: On the poisonous substance contained in holothurians. *Seto. Mar. Biol. Lab.* **4**, 183–203 (1995)
- Caulier, G., Mezali, K., Soualili, D.L., Decroo, C., Demeyer, M., Eeckhaut, I., Gerbaux, P., Flammang, P.: Chemical characterization of saponins contained in the body wall and the Cuvierian tubules of the sea cucumber *Holothuria (Platyperona) sanctori* (Delle Chiaje, 1823). *Biochem. Syst. Ecol.* **68**, 119–127 (2016)
- Kitagawa, I., Kobayashi, M.: On the structure of the major saponin from the starfish *Acanthaster Planci*. *Tetrahedron Lett.* **18**, 859–862 (1977)
- Demeyer, M., De Winter, J., Caulier, G., Eeckhaut, I., Flammang, P., Gerbaux, P.: Molecular diversity and body distribution of saponins in the sea star *Asterias rubens* by mass spectrometry. *Comp. Biochem. Physiol. B.* **168**, 1–11 (2014)
- Palagiano, E., Zollo, F., Minale, L., Iorizzi, M., Bryan, P., McClintock, J., Hopkins, T.: Isolation of 20 glycosides from the starfish *Henricia downeyae*, collected in the Gulf of Mexico. *J. Nat. Prod.* **59**, 348–354 (1996)
- Maier, M.S.: Biological activities of sulfated glycosides from echinoderms. *Stud. Nat. Prod. Chem.* **35**, 311–354 (2008)
- D'Auria, M.V., Minale, L., Riccio, R.: Polyoxygenated steroids of marine origin. *Chem. Rev.* **93**, 1839–1895 (1993)
- Van Dyck, S., Gerbaux, P., Flammang, P.: Qualitative and quantitative saponin contents in five sea cucumbers from the Indian ocean. *Mar. Drugs*. **8**, 173–189 (2010)
- Van Dyck, S., Gerbaux, P., Flammang, P.: Elucidation of molecular diversity and body distribution of saponins in the sea cucumber *Holothuria forskali* (Echinodermata) by mass spectrometry. *Comp. Biochem. Physiol. B.* **152**, 124–134 (2009)
- Shvartsburg, A.A., Jarrold, M.F.: An exact hard-spheres scattering model for the mobilities of polyatomic polyatomic ions. *Chem. Phys. Lett.* **261**, 86–91 (1996)
- Mesleh, M.F., Hunter, J.M., Shvartsburg, A.A., Schatz, G.C., Jarrold, M.F.: Structural information from ion mobility measurements: effects of the long-range potential. *J. Phys. Chem.* **100**, 16082–16086 (1996)
- Decroo, C., Colson, E., Lemaire, V., Caulier, G., De Winter, J., Cabrera-Barjas, G., Gerbaux, P.: Ion mobility mass spectrometry of saponin ions. *Rapid Commun. Mass Spectrom.* **33**(S2), 22–33 (2019)
- Decroo, C., Colson, E., Demeyer, M., Lemaire, V., Caulier, G., Eeckhaut, I., Gerbaux, P.: Tackling saponin diversity in marine animals by mass spectrometry: data acquisition and integration. *Anal. Bioanal. Chem.* **409**, 3115–3126 (2017)
- Patlolla, J.M.R., Rao, C.V.: Anti-inflammatory and anti-cancer properties of  $\beta$ -escin, a triterpene saponin. *Curr. Pharmacol. Rep.* **1**, 170–178 (2015)
- Abudayeh, Z.H.M., Al Azzam, K.M., Naddaf, A., Karpiuk, U.V., Kislichenko, V.S.: Determination of four major saponins in skin and endosperm of seeds of horse chestnut (*Aesculus hippocastanum* L.) using high performance liquid chromatography with positive confirmation by thin layer chromatography. *Adv. Pharm. Bull.* **5**, 587–591 (2015)
- Yoshikawa, M., Harada, E., Murakami, T., Matsuda, T., Wariishi, N., Yamahara, Y., Murakami, N., Kitagawa, I.: Escins-Ia, Ib, IIa, IIb, and IIIa, Bioactive triterpene oligoglycosides from the seeds of *Aesculus hippocastanum* L.: their inhibitory effects on ethanol absorption and hypoglycemic activity on glucose tolerance test. *Chem. Pharm. Bull.* **42**, 1357–1359 (1994)
- Yoshikawa, M., Murakami, T., Yamahara, J., Matsuda, H.: Bioactive saponins and glycosides. XII. Horse chestnut. (2): Structures of escins IIb, IV, V, and VI and isoescins Ia, Ib, and V, acylated polyhydroxyleanene triterpene oligoglycosides, from the seeds of horse chestnut tree (*Aesculus hippocastanum* L., *Hippocastanaceae*). *Chem. Pharm. Bull.* **46**, 1764–1769 (1998)

25. Yoshikawa, M., Murakami, T., Yamahara, J., Matsuda, H.: Bioactive saponins and glycosides. III. Horse chestnut. (1): the structures, inhibitory effects on ethanol absorption, and hypoglycemic activity of escins Ia, Ib, IIa, IIb, and IIIa from the seeds of *Aesculus hippocastanum* L. Chem. Pharm. Bull. **44**, 1754–1764 (1996)
26. Matsuda, H., Li, Y., Murakami, T., Ninomiya, K., Yamahara, J., Yoshikawa, M.: Effects of escins Ia, Ib, IIa, and IIb from horse chestnut, the seeds of *Aesculus hippocastanum* L., on acute inflammation in animals. Biol. Pharm. Bull. **20**, 1092–1095 (1997)
27. Duez, Q., Chirot, F., Liénard, R., Josse, T., Choi, C.M., Coulembier, O., Dugourd, P., Cornil, J., Gerbaux, P., De Winter, J.: Polymers for traveling wave ion mobility spectrometry calibration. J. Am. Soc. Mass Spectrom. **28**, 2483–2491 (2017)
28. Giles, K.; Ujma, J.; Wildgoose, J.; Green, M.; Richardson, K.; Langridge, D.; Tomczyk, N. Design and performance of a second-generation cyclic ion mobility enabled Q-TOF. June 6 (Poster Presentation). In: Proceedings of the 65th Conference on Mass Spectrometry and Allied Topics, Indianapolis in June 4–8 (2017);
29. Giles, K., Ujma, J., Wildgoose, J., Pringle, S., Richardson, K., Langridge, D., Green, M.: A cyclic ion mobility-mass spectrometry system. Anal. Chem. **91**, 8564–8573 (2019)
30. Smith, D., Knapman, T., Campuzano, I., Malham, R., Berryman, J., Radford, S., Ashcroft, A.: Deciphering drift time measurements from travelling wave ion mobility spectrometry-mass spectrometry studies. Eur. J. Mass Spectrom. **15**, 113 (2009)
31. Dodds, J.N., May, J.C., McLean, J.A.: Correlating resolving power, resolution, and collision cross section: unifying cross-platform assessment of separation efficiency in ion mobility spectrometry. Anal. Chem. **89**, 12176–12184 (2017)
32. Giles, K., Williams, J.P., Campuzano, I.: Enhancements in travelling wave ion mobility resolution. Rapid Commun. Mass Spectrom. **25**, 1559–1566 (2011)
33. Rathore, D., Dodds, E.D.: Collision-induced release, ion mobility separation, and amino acid sequence analysis of subunits from mass-selected noncovalent protein complexes. J. Am. Soc. Mass Spectrom. **25**, 1600–1609 (2014)